Proc. Indian Acad. Sci. (Earth Planet. Sci.), Vol. 89, Number 3, November 1980, pp. 277–292.

Monsoon cyclogenesis and large-scale flow patterns over South Asia

V SATYAN, R N KESHAVAMURTY*, B N GOSWAMI,**
S K DASH and H S S SINHA

Physical Research Laboratory, Navrangpura, Ahmedabad 380 009, India

* Present address : Geophysical Fluid Dynamics Program, Princeton University, Princeton, N.J. 08540, USA

** Present address : Goddard Space Flight Centre, Greenbelt, Md 20771, USA

MS received 2 June 1979 ; revised 5 May 1980

Abstract. An important problem of monsoon meteorology is understanding the mechanism of formation of monsoon disturbances over north Bay of Bengal. Using the linear stability analysis approach we have investigated in three different ways the stability of July mean monsoon zonal flow for the growth of disturbances. We have used a two-layer quasigeostrophic model and conducted combined barotropic-baroclinic stability analysis. In the first approach, we included cumulus heating into our model through CISK mechanism. We obtained growing modes in the lower troposphere. One of these modes has scale, structure and growth rate which agree well with those of the observed monsoon disturbances. In another study, we superposed a long stationary wave (the planetary monsoon wave) on the basic zonal flow and repeated the stability analysis. No heating was included in this case. This analysis also yielded growing disturbances in the basic flow. It turns out that one of these modes resembles well with the observed disturbances in respect of horizontal scale, growth rate and structure. Lastly, we examined the basic flow for instabilities when both cumulus heating and long wave are present. As expected there was enhancement in the growth rate and amplitude of perturbation as compared to their values in the earlier two cases. We have also studied the variability of monsoon cyclogenesis by considering the large-scale flow field over the monsoon region during active and break monsoon phases. We have conducted the above stability analysis of monsoon flow during break monsoon and just prior to disturbance formation. It is found that the flow during break monsoon is stable whereas the flow just prior to depression formation is found to be unstable and yields disturbances with realistic scales and growth rates.

Keywords. Monsoon cyclogenesis; monsoon variability; barotropic instability; baroclinic instability; cumulus heating; planetary monsoon wave; large scale flows.

1. Introduction

Among the major meteorological events taking place during a normal monsoon season the disturbances forming over north Bay of Bengal are perhaps the most interesting and important. The mechanism of formation of these disturbances

which can mature into large-scale depressions is as not yet completely understood. In the past, several studies have been made to understand this mechanism. The essential idea in these has been that the monsoon basic flow is unstable to small perturbations and the growing instabilities develop in the course of time into the observed disturbances. Both barotropic and baroclinic types of instabilities have been invoked as possible mechanisms for the growth of these disturbances. Keshavamurty (1971) suggested that baroclinic instability may not be the initial mechanism and stressed the role of conditional instability of the second kind (CISK) in the growth of monsoon disturbances. This is suggested by the fact that the monsoon atmosphere is conditionally unstable and there is always cyclonic vorticity present in the lower levels. Krishnamurthy *et al* (1975), from their study of the structure of a monsoon depression, have also suggested that CISK mechanism may be important. Shukla (1977) studied the barotropic-baroclinic instability of the monsoon wind field using a ten-layer quasigeostrophic model and found only an upper tropospheric growing mode at 150 mb. This was essentially a barotropic mode. Shukla (1978) also performed a CISK-barotropic-baroclinic instability analysis of monsoon flow by numerically integrating the linearised perturbation equations for a three-layer quasi-geostrophic model. He found that the maximum growth rate occurs for the smallest scales. The mechanism for scale selection was therefore not clear. Another approach to the monsoon cyclogenesis problem has been to include the basic meridional motion into the monsoon zonal flow and then see if this system yields growing modes when perturbed. Mak (1975) proposed that the baroclinic instability of the zonal flow over Western India with meridional motion included may be the growth mechanism for the middle tropospheric disturbances which form over this region. Further work in this regard may be found in Brode and Mak (1978). Satyan *et al* (1977) showed that the mean monsoon zonal flow with a long stationary wave superposed on it yields monsoon-like disturbances when subjected to perturbations. Recently, Frederiksen (1978) made a general study in which he examined the stability of planetary waves by themselves and together with zonal flows by an approach different from ours. He found that the zonal flows become unstable in the presence of planetary waves.

We describe in this paper our study of (i) monsoon cyclogenesis problem and (ii) the variability of cyclogenesis. First, we examine in detail the stability of the monsoon zonal flow (climatological July mean flow) using a combined barotropic-baroclinic model for the cases (i) when cumulus heating is included, (ii) when a long stationary wave (the planetary monsoon wave) is superposed on the basic zonal flow, and (iii) when both cumulus heating and the long wave are included. Secondly, the variability problem is studied by conducting combined barotropic-baroclinic stability analysis (with cumulus heating) of monsoon flow during break monsoon and just prior to disturbance formation.

2. Basic equations

We consider in our analysis the latitude channel between 5° N and 30° N over the longitude 80° E. We use a two-layer quasi-geostrophic model with beta-plane centred at the middle of the channel.

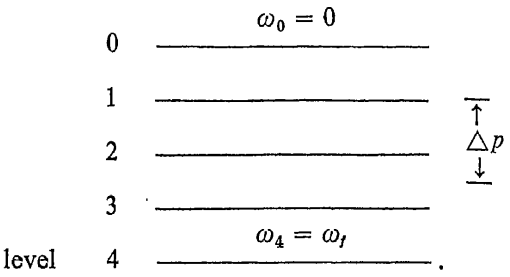

We consider at level 1 (200 mb) and level 3 (700 mb) the mean zonal flow over which is superposed the long stationary wave of the meridional wind component. Combined barotropic-baroclinic instability analysis of this system is performed by considering the linearised perturbation potential vorticity equations at levels 1 and 3 and the thermodynamic equation at level 2. Thus

$$\left[\frac{\partial}{\partial t} + U_1\frac{\partial}{\partial x} + \overline{v}_1^*\frac{\partial}{\partial y}\right]\left[\zeta_1' + \frac{S_2}{f_0}(\phi_3' - \phi_1')\right] + u_1'\left[\frac{\partial \overline{\zeta}_1^*}{\partial x} + S_2(\overline{v}_3^* - \overline{v}_1^*)\right] + v_1'\left[\beta - \frac{\partial^2 U_1}{\partial y^2} + \frac{\partial \overline{\zeta}_1^*}{\partial y} - S_2(U_3 - U_1)\right] = -\frac{S_2}{f_0}\frac{R}{C_p}\frac{\triangle p}{p}\dot{Q}_2' \tag{1}$$

$$\left[\frac{\partial}{\partial t} + U_3\frac{\partial}{\partial x} + \overline{v}_3^*\frac{\partial}{\partial y}\right]\left[\zeta_3' - \frac{S_2}{f_0}(\phi_3' - \phi_1')\right] + u_3'\left[\frac{\partial \overline{\zeta}_3^*}{\partial x} - S_2(\overline{v}_3^* - \overline{v}_1^*)\right] + v_3'\left[\beta - \frac{\partial U_3}{\partial y^2} + \frac{\partial \overline{\zeta}_3^*}{\partial y} + S_2(U_3 - U_1)\right] - f_0\frac{\omega_4'}{\triangle p} = \frac{S_2}{f_0}\frac{R}{C_p}\frac{\triangle p}{p}\dot{Q}_2' \tag{2}$$

where at levels 1 and 3, $U_1(y)$, $U_3(y)$ are mean zonal winds and v_1^*, $\overline{v}_3^*$ are stationary meridional winds. The latter are functions of y and they vanish at the southern and northern latitude boundaries. They have wave form like $\exp\{ik_{oj}x\}$ $(j = 1, 3)$ in the x-direction. The prime denotes perturbation : ϕ_i' is the perturbation geopotential, u_i', v_i' are the perturbation velocity components and ζ_i' is the perturbation vorticity. $\dot{Q}_2'$ is the rate of non-adiabatic perturbation heating at level 2 and f_0 is the constant coriolis parameter in the beta-plane approximation $f = f_0 + \beta y$. Further, $S_2 = f_0^2/\triangle p^2\sigma$ with

$$\triangle p = 500\,\text{mb}, \quad \sigma = -\frac{a}{\theta}\frac{\partial \theta}{\partial p}$$

where $a = -\partial\phi/\partial p$ and

$$\theta = T(p_0/p)^{R/c_p},$$

the potential temperature. In order to solve equations (1) and (2) we assume wave solutions of the type

$$\phi_j' = \phi_j(y)\exp\{ik(x - ct)\}, \quad j = 1, 3,$$

where the amplitude $\phi_j(y)$ and the phase velocity c can be complex. Substituting these solutions in equations (1) and (2) and carrying out the algebra, one gets

$$\left[ik(U_1 - c) + \bar{v}_1^* \frac{\partial}{\partial y}\right]\left[\frac{1}{f_0}\left(-k^2\phi_1 + \frac{\partial^2\phi_1}{\partial y^2}\right) + \frac{S_2}{f_0}(\phi_3 - \phi_1)\right]$$

$$-\frac{1}{f_0}\frac{\partial\phi_1}{\partial y}[-k_{01}^2\bar{v}_1^* + S_2(\bar{v}_3^* - \bar{v}_1^*)]$$

$$+\frac{ik}{f_0}\phi_1\left[\beta - \frac{\partial^2 U_1}{\partial y^2} + ik_{01}\frac{\partial\bar{v}_1^*}{\partial y} - S_2(U_3 - U_1)\right]$$

$$= -\frac{S_2}{f_0}\frac{R}{c_p}\frac{\triangle p}{p}\dot{Q}_2' \exp\{-ik(x - ct)\}$$

and

$$\left[ik(U_3 - c) + \bar{v}_3^* \frac{\partial}{\partial y}\right]\left[\frac{1}{f_0}\left(-k^2\phi_3 + \frac{\partial^2\phi_3}{\partial y^2}\right) - \frac{S_2}{f_0}(\phi_3 - \phi_1)\right]$$

$$-\frac{1}{f_0}\frac{\partial\phi_3}{\partial y}[-k_{03}^2\bar{v}_3^* - S_2(\bar{v}_3^* - \bar{v}_1^*)]$$

$$+\frac{ik}{f_0}\phi_3\left[\beta - \frac{\partial^2 U_3}{\partial y^2} + ik_{03}\frac{\partial\bar{v}_3^*}{\partial y} + S_2(U_3 - U_1)\right]$$

$$-\frac{f_0\omega_4'}{\triangle p} = \frac{S_2}{f_0}\frac{R}{c_p}\frac{\triangle p}{p}\dot{Q}_2' \exp\{-ik(x - ct)\}, \tag{4}$$

where k_{01} and k_{03} denote the wavenumber of the stationary monsoon waves (the planetary waves) at levels 1 and 3. The equations here are of third order and we have to specify three boundary conditions for their solutions. We first convert the equations into their finite difference forms and apply the backward difference formula at the northern latitude boundary and central difference formula at the southern boundary. The boundary conditions are

$\phi_1 = \phi_3 = 0$ at the southern latitude boundary,

$\partial\phi_1/\partial y = \partial\phi_3/\partial y = 0$ at the northern latitude boundary,

and $\omega_0 = 0$ at the top boundary and $\omega_4 = \omega_f$, the frictional ω at the bottom boundary. The frictional ω_f is given by (Charney and Eliassen 1964)

$$\omega_f = -g\rho w,$$

$$= -g\rho \cdot \tfrac{1}{2} D_E a \zeta_g \sin 2\alpha,$$

$$\zeta_g = \frac{1}{f_0}\nabla^2\phi_3 \exp\{ik(x - ct)\}$$

where the different symbols have their usual meaning. The factor a is taken to be 0·8 so that the geostrophic vorticity at the bottom boundary is 0·8 times its value at the surface. We get

$$\frac{f_0}{\triangle p}\omega_4' = -\frac{1}{f_0}ag\rho \sin 2\alpha\,(Kf_0/2)^{1/2}\left\{-k^2\phi_3 + \frac{\partial^2\phi_3}{\partial y^2}\right\}$$

$$\times \exp\{ik(x - ct)\}.$$

Assuming that CISK type heating is important for the growth of disturbances we adopt here a simple parameterisation scheme (Ooyama 1964, 1972; Charney and Eliassen 1964) for the convective heating on the right side of equations (3) and (4). We can write this term as

$$\frac{\Delta p}{p}\frac{S_2}{f_0}\frac{R}{c_p}\dot{Q}_2$$

$$= \frac{1}{f_0}\frac{g\rho}{\Delta p}\sin 2a\,(Kf_0/2)^{1/2}\,a\,H(p)\left[-k^2\phi_3 + \frac{\partial^2\phi_3}{\partial y^2}\right]\exp\{ik(x-ct)\}$$

after we have substituted for $\dot{Q}_2$:

$$\dot{Q}_2 = -H(p)\,c_p\left(\frac{p}{p_0}\right)^{R/c_p}\cdot\left(-\frac{\partial\theta}{\partial p}\right)\omega_f,$$

where $H(p)$ is the vertical distribution function for the heating. We have assumed a constant value of 1·5 for $H(p)$ in the present analysis. It should be mentioned here that in our calculations the heating is switched on only when the vertical shear of the zonal wind is less than 22 meter/sec. This condition on allowing heating is based on observations of wind shear in the vertical during breaks and just before the formation of depressions. We have used a value of 22 meter/sec which is valid for the region around 19° N.

From the difference scheme for the differential equations (3) and (4) one obtains a system of linear algebraic equations which can be solved by employing the standard techniques for finding eigenvalues. In the present case there are $2N$ equations in $2N$ unknowns (for a given grid of $N+2$ points at each of the levels 1 and 3) and for a non-trivial solution the determinants of their coefficients must vanish. In the matrix notation one has

$$(P - cQ)\,\phi = 0,$$

or $$(Q^{-1}P - cI)\,\phi = 0,$$

where the matrices P, Q have their usual meaning (Keshavamurty *et al* 1978a). ϕ is the geopotential and c is the complex phase speed. Note that in the present case the matrix P is complex. The problem thus reduces to the diagonalisation of the matrix $Q^{-1}P$. This is done using a standard matrix diagonalisation routine on a computer.

3. Results and discussion

The stability analysis described in § 2 was carried out for monsoon flows using July mean wind profiles over the region of 80° E longitude. The latitudinal profiles of the zonal wind field at 700 mb and 200 mb levels are shown in figures 1 and 2 respectively. We considered the following three cases :

(i) Stability analysis with cumulus heating included using the simple CISK parameterisation scheme described in § 2. The relevant equations in this case are obtained by dropping the terms containing $\overline{v}_1^*$, $\overline{v}_3^*$ in equations (3) and (4).

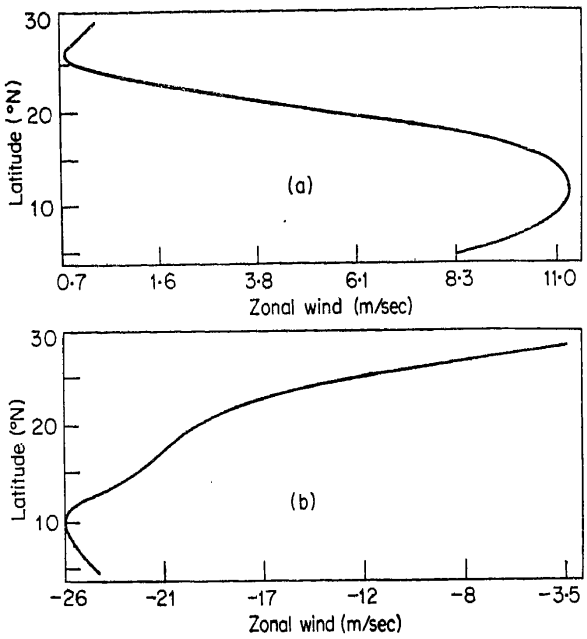

Figure 1. (a) Mean zonal wind profile over 80° E during July at 700 mb. (b) Mean zonal wind profile over 80° E during July at 200 mb.

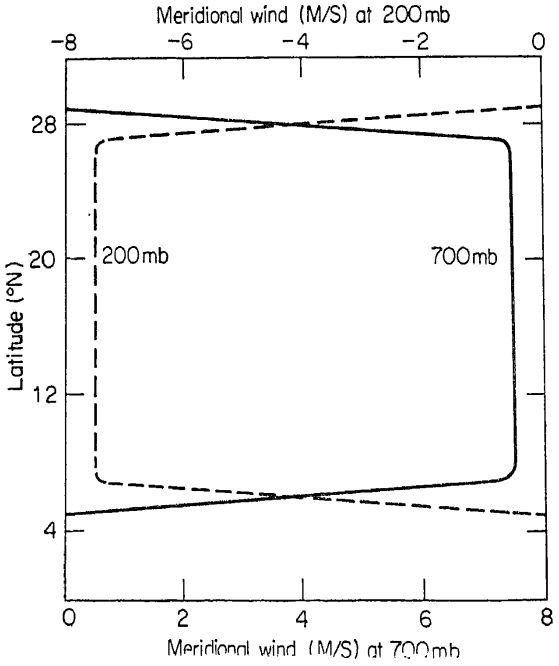

Figure 2. Meridional wind profile at 700 and 200 mb.

(ii) Stability analysis with the meridional wind component included as part of a long stationary wave.

(iii) Stability analysis with both cumulus heating and the meridional wind included.

The characteristics of the growing modes in the upper troposphere are given in table 1. It is seen that in all the three cases mentioned above, the upper level flow is unstable and yields rapidly propagating disturbances. These may be compared with the easterly waves one observes in the upper troposphere. Growing mode characteristics for the lower troposphere are given in table 2. These results are for the case (i). Figure 3 (a) shows the variation of doubling time with wavelength for the different growing modes. We see that the fastest growing lower tropospheric mode has a doubling time of 3·5 days and its wavelength is about

Table 1. Characteristics of upper tropospheric growing modes—combined barotropic-baroclinic instability of mean zonal flow during July over 80° E.

	Horizontal scale length (km)	Phase speed (meter/sec)	Doubling time (days)	Maximum amplitude			
				200 mb		700 mb	
				Strength	Position °N	Strength	Position °N
With heating	3000	−25·1	7·1	340	13	10	15
With meridional wind	2400	−17·4	1·8	420	22	115	8
With heating and meridional wind	3000	−16·0	2·2	400	22	220	9

Table 2. Characteristics of lower tropospheric growing modes—combined barotropic-baroclinic instability (with heating) of mean zonal flow during July over 80° E.

Horizontal scale length (km)	Phase speed (meter/sec)	Doubling time (days)	Maximum amplitude			
			700 mb		200 mb	
			Strength	Position °N	Strength	Position °N
2000	1·2	7·8	280	22	16	22
2200	1·3	7·8	400	22	24	22
2400	1·5	5·1	420	22	25	22
2600	1·4	4·0	440	21	28	21
2800	1·2	3·6	470	20	32	20
3000	1·1	3·5	492	19	35	20
3200	0·8	3·5	560	19	41	20
3400	0·6	3·6	650	19	49	19
3600	0·3	3·7	740	18	59	18
3800	0·1	4·1	830	18	69	18
4000	−0·2	5·0	940	18	80	18

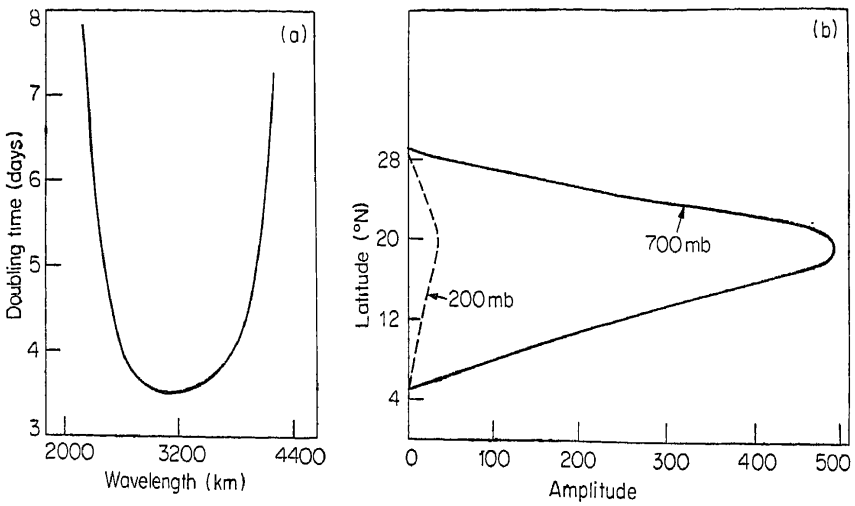

Figure 3. (a) Growth rate, wavelength diagram, and combined barotropic-baroclinic instability (with heating) of mean zonal flow for July. (b) Amplitude structure of the fastest growing disturbance of figure 3 (a).

3000 km. Figure 3 (b) shows the amplitude structure of this most unstable mode. This mode has maximum amplitude around 19° N latitude in which latitude region the observed monsoon disturbances are most often formed. The phase speed of the disturbance is about 1 meter/sec which is of the same order as the speed of the observed disturbances. This disturbance, however, moves in an eastward direction unlike the majority of observed disturbances which move westward. Comparing these results with our earlier result of combined barotropic-baroclinic instability (without heating) of mean zonal flow during July over 80° E (Goswami *et al* 1980) we conclude that barotropic instability in the presence of cumulus heating plays an important role in the growth of monsoon disturbances.

Next, by superposing a long stationary wave (the planetary monsoon wave) on the mean zonal flow we included the meridional component of wind into our basic state. Cumulus heating was not included in this case. The latitudinal profiles of the meridional wind component (the v-wave) at levels 700 mb and 200 mb are shown in figure 3. It is chosen to be southerly in the lower level and northerly in the upper level with a constant amplitude of 7·5 meter/sec in each case. Further, its amplitude vanishes at the two ends of the latitude channel. We ensure by choosing such a profile that the flow is nondivergent in most parts of the latitudinal channel except near the boundaries where the gradient of meridional wind is not zero. In our computations we have also set to zero the $\partial\bar{v}^*/\partial y$ terms in equations (3) and (4). The v-waves are taken to be 180° longitude in length so that they represent the dominant component of the observed planetary monsoon field (Krishnamurti 1971) which has the same scale length. It should be mentioned here that it is essential that the long wave sits over the Indian longitudes with a proper phase. The crucial role of this phase in inducing or inhibiting cyclogenesis has been discussed elsewhere (Keshavamurty *et al* 1978b). The results of our analysis are shown in table 3, figures 4 (a, b). It is clear from table 3 that the lower tropospheric flow is unstable. We see that the most unstable

Table 3. Characteristics of lower tropospheric growing modes—combined barotropic baroclinic instability (with meridional wind) of mean zonal flow during July over 80° E.

Horizontal scale length (km)	Phase speed (meter/sec)	Doubling time (days)	Maximum amplitude			
			700 mb		200 mb	
			Strength	Position °N	Strength	Position °N
2000	−5·1	6·5	180	22	270	25
2200	−3·4	6·6	240	21	270	25
2400	−3·9	4·5	260	21	340	25
2600	−5·4	3·5	240	21	380	25
2800	−4·2	3·6	350	10	380	25
3000	−3·0	3·8	420	13	360	23
3200	−1·8	4·1	460	14	350	23
3400	−0·6	4·4	450	14	360	24
3600	0·6	4·7	430	14	350	24
3800	1·8	5·0	400	13	345	25
4000	3·1	5·1	390	13	345	24

mode has a doubling time of 3·5 days and its horizontal scale is about 2600 km. Its amplitude maximum is quite pronounced and is situated around 21° N. Furthermore, this is a westward moving disturbance with a speed of 5·4 meter/sec. We identify this mode as a monsoon disturbance since it closely resembles in synoptic features the observed disturbances in this longitude-latitude region.

In view of the above findings one would expect that when both cumulus heating and meridional wind component are present, the combined barotropic-baroclinic instability of the zonal flow would be much more pronounced. We therefore repeated the stability analysis calculations incorporating both heating and v-wave and the results indeed confirmed this. These results are given in table 4. The growth rate diagram and the amplitude structure are shown in figures 5 (a, b). We find that the fastest growing mode is 3000 km long, is moving westward at 5·7 meter/sec, and its amplitude doubles in 1·8 days. We conclude that cumulus heating and v-wave act coherently in inducing growth of disturbances in this region.

4. Large-scale flow patterns over South Asia and monsoon cyclogenesis

4.1. *Introduction*

The South Asian summer monsoon circulation, as well as the associated rainfall, show considerable fluctuations during a season as well as from year to year and presumably even on the longer time scales of climatic changes. During a monsoon season there are periods of sustained monsoon activity when a series of monsoon disturbances form over the north Bay of Bengal and also mid-tropospheric

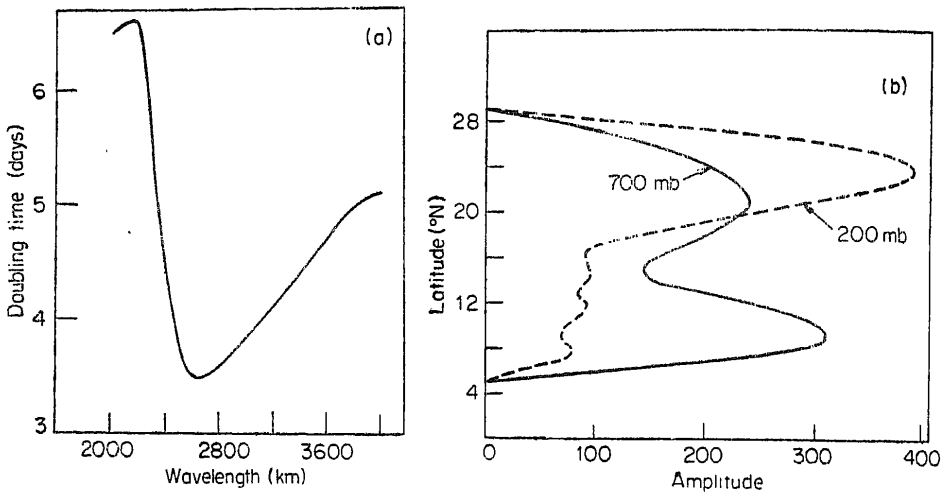

Figure 4. (a) Growth rate, wavelength diagram and combined barotropic-baroclinic instability (with meridional wind) of mean zonal flow for July. (b) Amplitude structure of the fastest growing disturbance of figure 4 (a).

disturbances form over the Gujarat region and we have well-distributed rains over central and adjoining north and west India. Often the monsoon trough from northwest India to northwest Pacific is active with a number of disturbances embedded in it. Figure 6 shows the time evolution of a composite of cases of active monsoon situations. The details of the compositing are described in Alexander *et al* (1977). The most notable feature is the east-west anomaly shear zone in the lower and middle tropospheres which progresses from the latitudes of peninsular India to north India. Most often these are associated with disturbances.

During breaks, on the other hand, we have anticyclonic flow (anomalous) in the lower troposphere and this also progresses northwards with the progress of the break (figure 7). When this anomalous anticyclonic flow is superposed on the mean monsoon flow, it results in the well-recognised synoptic feature—the strong low level westerlies over the peninsula shift northwards.

The number and tracks of monsoon disturbances also show year-to-year variability (Ramamurthy 1969). During prolonged breaks, these disturbances either fail to form or even if they form, they move northwest or northwards. One would suspect that the large-scale changes in monsoon circulation would affect disturbance formation and hence monsoon rainfall. We test this idea by conducting stability analysis of monsoon zonal flow corresponding to average break conditions and conditions just prior to disturbance formation.

4.2. *Results and discussion*

We repeated the instability analysis. viz., combined barotropic-baroclinic instability analysis (with heating) with zonal flow corresponding to (i) average break conditions (figures 8 (a, b)), and (ii) to average conditions one day before depression formation (figure 9 (a, b)). The flow profiles were constructed using the mean zonal

Table 4. Characteristics of lower-tropospheric growing modes—combined barotropic-baroclinic instability (with heating and meridional wind) of mean zonal flow during July over 80° E.

Horizontal scale length (km)	Phase speed (meter/sec)	Doubling time (days)	Maximum amplitude			
			700 mb		200 mb	
			Strength	Position °N	Strength	Position °N
2000	−3·4	4·5	480	23	230	26
2200	−5·0	4·0	470	23	260	24
2400	−3·8	3·6	560	22	320	24
2600	−6·9	2·9	480	23	350	24
2800	−6·2	2·1	380	22	390	23
3000	−5·7	1·8	340	20	400	23
3200	−5·1	1·9	460	15	360	23
3400	−4·1	2·0	560	15	320	23
3600	−3·2	2·0	550	15	350	23
3800	−2·4	2·0	530	15	390	23
4000	−1·5	2·1	500	14	400	23

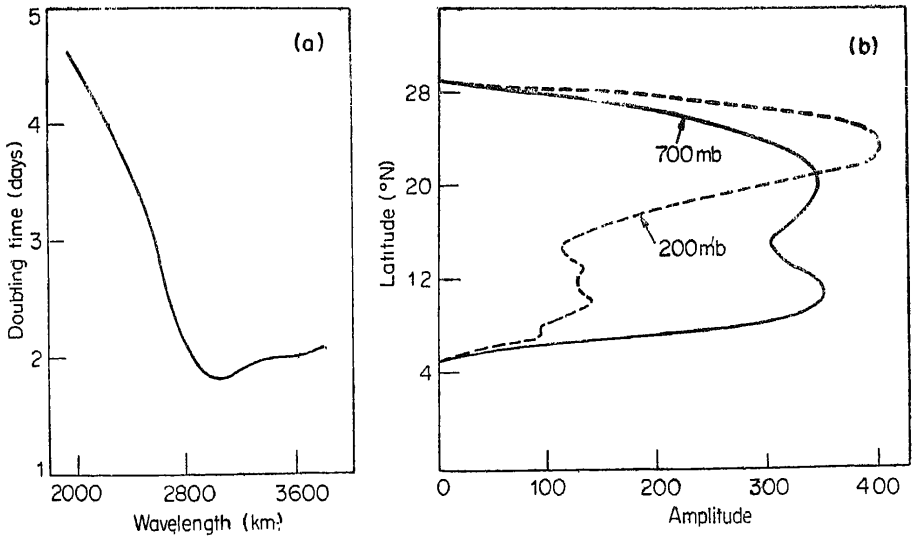

Figure 5. (a) Growth rate, wavelength diagram and combined barotropic–baroclinic instability (with heating and meridional wind) of mean zonal flow for July. (b) Amplitude structure of the fastest growing disturbance of figure 5 (a).

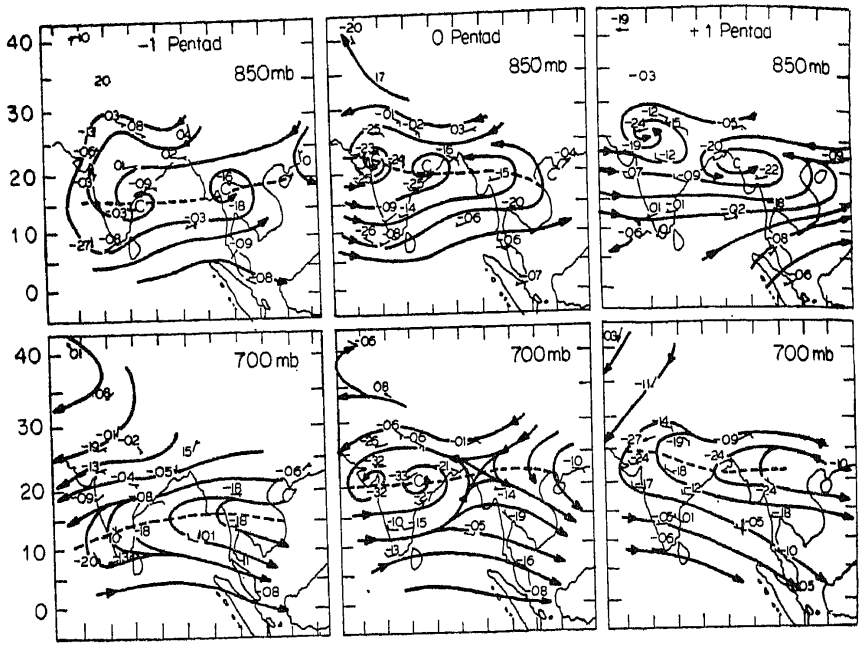

Figure 6. Composite wind, contour anomalies and streamlines during the peak 5 day period of strong monsoon activity and one pentad before and after at 850 and 700 mb.

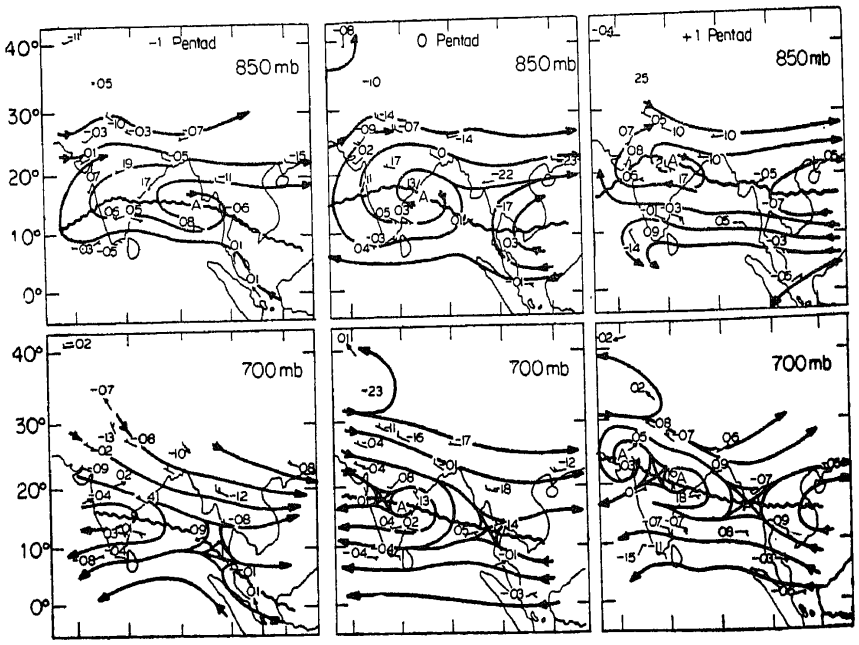

Figure 7. Composite wind, contour anomalies and streamlines during the peak 5-day period of break monsoon and one pentad before and after at 850 and 700 mb.

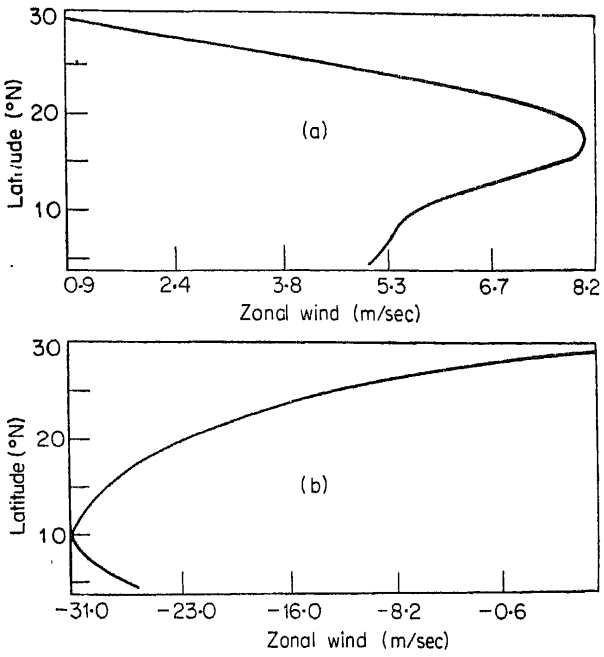

Figure 8. (a) Mean zonal wind profile during break at 700 mb. (b) Mean zonal wind profile during break at 200 mb.

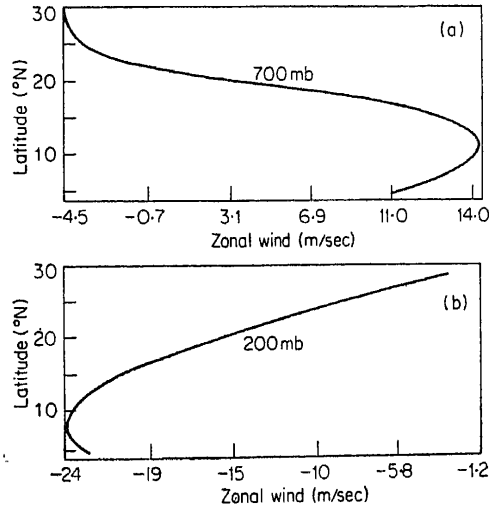

Figure 9. (a) Mean zonal wind profile one day before depression formation at 700 mb. (b) Mean zonal wind profile one day before depression formation at 200 mb.

winds (during July) for normal monsoon seasons, the composite transient disturbance charts for the day before the day of depression formation, and the anomaly field during breaks (Keshavamurty *et al* 1978a). When we conducted the stability analysis with flow corresponding to breaks the flow was found to be stable. On the other hand, the flow prior to depression formation yielded disturbances with a faster growth rate than in the case of mean monsoon flow. Table 5 gives

Table 5. Characteristics of lower tropospheric growing modes—combined barotropic-baroclinic instability (with heating) of zonal flow corresponding to average conditions one day before depression formation during July over 80° E.

Horizontal scale length (km)	Phase speed (meter/sec)	Doubling time (days)	Maximum amplitude			
			700 mb		200 mb	
			Strength	Position °N	Strength	Position °N
1800	4·3	3·9	200	19	3·5	19
2000	4·3	3·4	220	20	4·0	19
2200	4·2	3·1	230	20	4·3	20
2400	4·2	3·0	240	20	4·7	20
2600	4·1	2·9	250	18	5·3	21
2800	4·1	2·9	250	19	6·0	21
3000	4·0	3·1	260	18	7·0	21
3200	3·9	3·2	260	17	9·0	21
3400	3·9	3·4	260	16	10·0	21
3600	3·8	3·6	260	17	12·0	20

the characteristics of the different growing modes. Figure 10 (a) shows the growth rates of the disturbances plotted against their wavelengths. From this we see that the fastest growing mode has a horizontal scale length of about 2500 km and doubling time of 2·9 days. The phase speed of this mode is about 4 meter/sec. Figure 10 (b) shows the amplitude structure of this disturbance. The amplitude is maximum around 19° N latitude.

These differences in the stability characteristics of the monsoon flow field during active and break monsoon discussed above arise probably from two physical causes :

(i) During breaks the meridional shear of the zonal wind reduces considerably and thus leads to less chances of barotropic instability.

(ii) The anticyclonic shear in the friction layer extending to almost 18–20° N during breaks would inhibit cumulus convection and thus preclude growth by the CISK mechanism.

5. Conclusions

Combined barotropic-baroclinic stability analyses of monsoon zonal flow using July mean flow profiles over 80° E longitude have been carried out using a two-layer quasigeostrophic model. Three cases were considered, viz., stability analysis (i) with cumulus heating, (ii) with meridional wind component as part of a long stationary wave superposed on the zonal flow, and (iii) with both cumulus heating and long wave present. In each case the zonal flow in the upper and lower

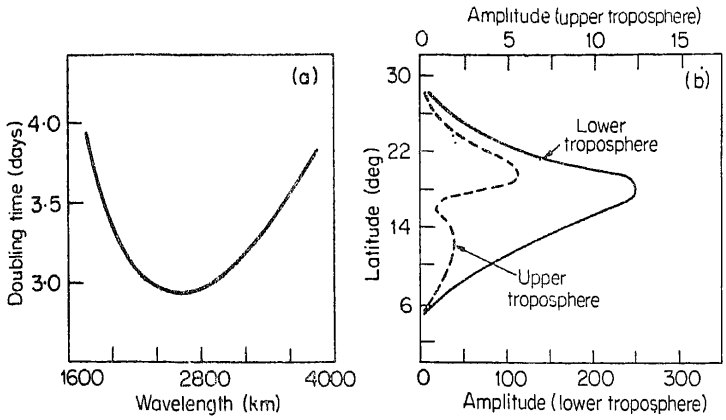

Figure 10. (a) Growth rate, wavelength diagram and combined barotropic–baroclinic instability with heating of average zonal flow one day before depression formation. (b) Amplitude structure of the fastest growing disturbance of figure 10(a).

troposphere was unstable. The unstable modes in the upper layer are found to resemble the observed easterly waves. The growing modes in the lower troposphere compare well with observed monsoon disturbances in horizontal scale length, growth rate phase speed and amplitude structure. It is concluded that inclusion of cumulus heating and/or meridional wind into the mean zonal flow can induce cyclogenesis.

Having identified the probable physical mechanisms inducing cyclogenesis these ideas are then extended to study the effect of large-scale changes in the monsoon circulation on disturbance formation and hence monsoon rainfall. This is done by conducting stability analysis of monsoon zonal flow corresponding to average break conditions and conditions just a day prior to depression formation. It is found that the flow during break monsoon is stable whereas the flow a day before the depression formation is found to be unstable and yields disturbances with realistic scales and growth rates. Two probable physical causes responsible for the differences in the stability characteristics of monsoon flow field during these contrasting situations are indicated.

References

Alexander G, Keshavamurty R N, De U S, Chellappa R, Das S K and Pillai P V 1977 Proc. Int. Symp. Monsoons 1978 India, New Delhi, *Indian J. Meteorol. Hydrol. Geophys.* **29** 76

Brode R W and Mak Mankin 1978 *J. Atmos. Sci.* **35** 1473

Charney J G and Eliassen A 1964 *J. Atmos. Sci.* **21** 68

Frederiksen J S 1978 *Q. J. R. Meterol. Soc.* **104** 841

Goswami B N, Keshavamurty R N, and Satyan V 1920 *Proc. Indian Acad. Sci. (Earth and Planet. Sci.)* **A89** 79

Keshavamurty R N 1971 On the maintenance of the mean Indian Southwest monsoon circulation and the structure and the energetics of the monsoon disturbances ; *Ph.D. Thesis* Mysore University.

Keshavamurty R N, Asnani G C, Pillai P V and Das S K 1978a *Proc. Indian Acad. Sci. (Earth Planet. Sci.)* **A87** 61

Keshavamurty R N, Satyan V and Goswami B N 1978b *Nature (London)* **274** 576

Krishnamurty T N 1971 *J. Atmos. Sci.* **28** 1342

Krishnamurty T N, Godbole R, Chang C B, Carr F and Chow J 1975 *J. Meteorol. Soc. Jpn.* Ser. II **53** 227

Mak M K 1975 *J. Atmos. Sci.* **32** 2246

Ooyama K 1964 *Geofisica. International,. Mexico* **4** 187

Ooyama K 1972 *Meteor. Soc.* **49** 744

Ramamurthy K 1969 Forecasting Manual No. IV-18·3, p. 57, India Meteorological Department, Pune, India

Satyan V, Keshavamurty R N and Goswami B N 1977 Proc. of IUTAM/IUGG Symposium on Monsoon Dynamics (New Delhi, December 1977) *Monsoon Dynamics* eds. James Lighthill and R P Pearce (Cambridge : University Press)

Shukla J 1977 *Pure Appl. Geophys.* **115** 1449

Shukla J 1978 *J. Atmos. Sci.* **35** 495